BIOCHEMISTRY
including biophysical chemistry & molecular biology
Article

Biochemistry **2010,** *49,* 8415–8424 8415
DOI: 10.1021/bi1009024

In Vitro Bypass of the Major Malondialdehyde- and Base Propenal-Derived DNA Adduct by Human Y-family DNA Polymerases κ, ι, and Rev1[†]

Leena Maddukuri,[‡] Robert L. Eoff,[‡] Jeong-Yun Choi,[‡,∥] Carmelo J. Rizzo,[‡,§] F. Peter Guengerich,[‡] and Lawrence J. Marnett*[,‡,§]

[‡]*A. B. Hancock Jr. Memorial Laboratory for Cancer Research, Departments of Biochemistry,* [§]*Chemistry and Pharmacology, Center in Molecular Toxicology, Vanderbilt Institute of Chemical Biology, and Vanderbilt-Ingram Cancer Center, Vanderbilt University School of Medicine, Nashville, Tennessee 37232-0146, and* [∥]*Department of Pharmacology, School of Medicine, Ewha Womans University, 911-1 Mok-5-Dong, Yangcheon-Gu, Seoul 158-710, Republic of Korea*

Received June 3, 2010; Revised Manuscript Received August 4, 2010

ABSTRACT: 3-(2′-Deoxy-β-D-*erythro*-pentofuranosyl)pyrimido-[1,2-*a*]purin-10(3*H*)-one (M_1dG) is the major adduct derived from the reaction of DNA with the lipid peroxidation product malondialdehyde and the DNA peroxidation product base propenal. M_1dG is mutagenic in *Escherichia coli* and mammalian cells, inducing base-pair substitutions (M_1dG → A and M_1dG → T) and frameshift mutations. Y-family polymerases may contribute to the mutations induced by M_1dG *in vivo*. Previous reports described the bypass of M_1dG by DNA polymerases η and Dpo4. The present experiments were conducted to evaluate bypass of M_1dG by the human Y-family DNA polymerases κ, ι, and Rev1. M_1dG was incorporated into template-primers containing either dC or dT residues 5′ to the adduct, and the template-primers were subjected to *in vitro* replication by the individual DNA polymerases. Steady-state kinetic analysis of single nucleotide incorporation indicates that dCMP is most frequently inserted by hPol κ opposite the adduct in both sequence contexts, followed by dTMP and dGMP. dCMP and dTMP were most frequently inserted by hPol ι, and only dCMP was inserted by Rev1. hPol κ extended template-primers in the order M_1dG:dC > M_1dG:dG > M_1dG:dT ∼ M_1dG:dA, but neither hPol ι nor Rev1 extended M_1dG-containing template-primers. Liquid chromatography−mass spectrometry analysis of the products of hPol κ-catalyzed extension verified this preference in the 3′-GXC-5′ template sequence but revealed the generation of a series of complex products in which dAMP is incorporated opposite M_1dG in the 3′-GXT-5′ template sequence. The results indicate that DNA hPol κ or the combined action of hPol ι or Rev1 and hPol κ bypass M_1dG residues in DNA and generate products that are consistent with some of the mutations induced by M_1dG in mammalian cells.

Endogenous DNA damage is a key event contributing to human diseases such as cancer and neurodegeneration (*1*−*3*). Lipid peroxidation and DNA peroxidation are major sources of endogenous DNA damage (*4*, *5*). M_1dG[1] (3-(2′-deoxy-β-D-*erythro*-pentofuranosyl)pyrimido-[1,2-*a*]purin-10(3*H*)-one) is a member of a unique class of endogenous DNA adducts that are derived from electrophiles generated by both lipid peroxidation and DNA peroxidation (Figure 1) (*6*, *7*). In this regard, DNA peroxidation appears to be a particularly important source of M_1dG (*8*). M_1dG adducts have been detected routinely in healthy humans at levels of ∼1−4 adducts per 10^8 nucleotides (*9*−*12*). Structural studies reveal that when placed in duplex DNA, opposite to dC, M_1dG undergoes hydrolytic ring opening to N^2-(3-oxo-1-propenyl)-2′-deoxyguanosine (N^2-OPdG) (Figure 1) (*13*, *14*). Both M_1dG and OPdG are mutagenic in bacteria (*Escherichia coli*) and mammalian cells (COS-7), but the mutation frequency induced by M_1dG is higher than N^2-OPdG (*15*, *16*). The types of mutations induced by M_1dG in site-specific mutagenesis experiments include base pair substitutions (M_1dG → A ∼ T > C), frameshifts, and

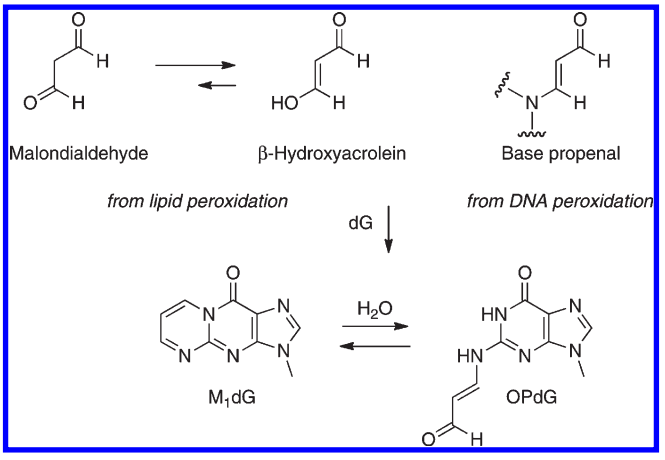

FIGURE 1: Schematic representation of pathways generating M_1dG and/or N^2-OPdG adducts.

[†]This work was supported by research grants from the National Institutes of Health [R37 CA087819 (L.J.M.), K99 GM084460 (R.L.E.), R01 ES10375 (F.P.G.), and P30 ES000267 (F.P.G., L.J.M.)].

*To whom correspondence should be addressed at the Department of Biochemistry, Vanderbilt University School of Medicine. E-mail: larry.marnett@vanderbilt.edu. Telephone: 615-343-7329. Fax: 615-343-7534.

[1]Abbreviations: M_1dG, 3-(2′-deoxy-β-D-*erythro*-pentofuranosyl)pyrimido-[1,2-*a*]purin-10(3H)-one; hPol κ, human DNA polymerase kappa; hPol ι, human DNA polymerase iota; BSA, bovine serum albumin; DTT, dithiothreitol; EDTA, ethylenediaminetetraacetic acid; HPLC, high-performance liquid chromatography; UPLC, ultraperformance liquid chromatography; LC-MS/MS, liquid chromatography−tandem mass spectrometry; MDA, malondialdehyde; MOPS, 3-morpholinopropane-1-sulfonic acid; PAGE, polyacrylamide gel electrophoresis; ds, double stranded; ss, single stranded; UDG, uracil DNA glycosylase.

Published on Web 08/20/2010

untargeted mutations (*15*, *16*). The polymerases responsible for M_1dG mutagenesis have not been unequivocally identified in mammalian cells, but the error-prone DNA polymerase V plays an important role in *E. coli* (*15*).

In the past decade, a specialized class of DNA polymerases called Y-family polymerases has been discovered in both prokaryotic, archaeal, and eukaryotic organisms (*17*−*19*). These polymerases are capable of bypassing a large variety of DNA lesions with low efficiency and fidelity (*20*, *21*). Humans express five translesion DNA polymerases, four belonging to the Y-family, Pol η, Pol ι, Pol κ, and Rev1 (*18*, *22*), and one B-family member, Pol ζ (*23*).

Recent studies show that both hPol η and Dpo4 (an archeal homologue of hPol κ) perform translesion DNA synthesis on templates containing M_1dG. Replication is error-prone and results in the insertion of dAMP opposite the adduct or insertion of dNMP opposite the 5′-template base to generate a one-base deletion (*24*, *25*). The insertion of dAMP opposite M_1dG leads to the occurrence of M_1dG → dT transversions in the second round of replication. Previous studies establish that M_1dG induces both transition and transversion mutations at similar frequencies in COS-7 cells so it is possible that multiple translesion polymerases are responsible for its mutation spectrum (*16*). Thus, in the present study we investigated the ability of hPol κ, hPol ι, and Rev1 to perform translesion DNA synthesis on a template-primer containing a single M_1dG adduct. Our results indicate that all three polymerases are able to insert dNMPs opposite M_1dG but that Rev1 and hPol ι are more efficient than hPol κ at inserting dCMP opposite the lesion. In contrast, and as reported earlier for related exocyclic DNA adducts (*26*−*28*), hPol κ is able to extend past M_1dG whereas hPol ι and Rev1 are not. The results of the experiments suggest Pol ι, Rev1, and Pol κ may cooperate in bypassing M_1dG residues and may introduce mutations that are observed in cellular mutagenesis experiments.

MATERIALS AND METHODS

Materials. Full-length recombinant hPol κ and hPol ι were purchased from Enzymax (Lexington, KY). T4 polynucleotide kinase and *E. coli* uracil DNA glycosylase were obtained from New England Biolabs (Beverly, MA). [γ-^{32}P]ATP was purchased from Perkin-Elmer. Core hPol κ (aa 19−526) and full-length Rev1 proteins were prepared as described previously (*29*, *30*).

Oligonucleotide Synthesis. The M_1dG-containing oligonucleotides were synthesized by a postsynthetic modification strategy as described previously and purified by HPLC (*19*). The unmodified oligonucleotides (HPLC-purified) were purchased from integrated DNA technologies (Coralville, IA). The sequences of the oligonucleotides are shown in Table 1.

Generation of Primer-Template DNA Substrates for in Vitro Assays. The 18-mer primer oligonucleotide was 5′-phosphorylated with T4 polynucleotide kinase in the presence of 250 μCi of [γ^{32}-P]ATP (>6000 Ci/mmol), 50 mM Na-MOPS buffer (pH 7.5), 10 mM $MgCl_2$, and 5 mM DTT for 1 h at 37 °C. The 23-mer templates containing either dG or M_1dG were annealed with radioactively labeled 18-mer primers (1:1 molar ratio) and heated to 95 °C for 3 min, followed by slow cooling overnight.

Primer Extension and Single Nucleotide Insertion Assays. Primer extension and individual nucleotide insertion reactions for M_1dG-containing substrates were conducted at 37 °C in 20 μL of buffered solutions containing 50 mM Na-MOPS (pH 7.5), 5 mM $MgCl_2$, 5 mM DTT, 10 μg of BSA, 10% glycerol (v/v), 50 nM primer-template complexes, and 500 μM dNTP mix (all four dNTPs) or 500 μM individual dNTPs (dATP, dCTP, dGTP, or dTTP). Polymerases were added to the following final concentation: 5 nM of hPol κ, hPol ι, or hRev1. Corresponding unmodified primer/template complexes were extended as controls, and the reaction conditions for the unmodified DNA substrates were the same as those for the modified templates. The reactions were quenched after preselected time intervals (0−120 min) by the addition of 6 μL of stop solution (10 mM EDTA, 95% formamide (v/v), 0.03% bromophenol blue (w/v), 0.03% xylene cyanol (w/v)) to a 4 μL aliquot of the sample. Reaction products were separated by gel electrophoresis (20% (w/v) denaturing polyacrylamide gel containing 7 M urea) at a constant voltage (2500 V) for 3 h. The radioactive products were then visualized using a phosphorImager and quantified using Quantity One software.

Table 1: DNA Substrate Sequences[a]

substrates used in insertion and extension assays	
5′-GGG GGC TCG TAA GGA TTC-3′	
3′-CCC CCG AGC ATT CCT AAG **XC**A CT-5′	substrate 1
5′-GGG GGC TCG TAA GGA TTC-3′	
3′-CCC CCG AGC ATT CCT AAG **XT**A CT-5′	substrate 2
5′-GGG GGC TCG TAA GGA TTC **C**-3′	
3′-CCC CCG AGC ATT CCT AAG **XC**A CT-5′	substrate 3
5′-GGG GGC TCG TAA GGA TTC **A**-3′	
3′-CCC CCG AGC ATT CCT AAG **XC**A CT-5′	substrate 4
5′-GGG GGC TCG TAA GGA TTC **G**-3′	
3′-CCC CCG AGC ATT CCT AAG **XC**A CT-5′	substrate 5
5′-GGG GGC TCG TAA GGA TTC **T**-3′	
3′-CCC CCG AGC ATT CCT AAG **XC**A CT-5′	substrate 6
substrates used only in LC-MS analysis	
5′-GGG GGA AGG AUT C-3′	
3′-CCC CCT TCC TAA G**XC** ACT-5′	substrate 7
5′-GGG GGA AGG AUT C-3′	
3′-CCC CCT TCC TAA G**XT** ACT-5′	substrate 8

[a] **X** denotes G or M_1dG.

Steady-State Kinetic Analysis. Steady-state kinetic reactions were performed for both unadducted or single M_1dG adducted substrates in the presence of 50 mM Na-MOPS buffer (pH 7.5), 50 mM NaCl, 5 mM DTT, 5 mM $MgCl_2$, 100 μg/mL BSA, 5% glycerol (v/v), 50 nM annealed 5′-end-labeled primer-template, 5 nM hPol κ, hPol ι, or Rev1, and varying concentrations of individual dNTPs (0−800 μM). Samples were incubated at 37 °C for different time periods. Reactions were terminated by addition of 36 μL of 95% formamide (w/v), 10 mM EDTA, 0.03% bromophenol blue (w/v), and 0.03% xylene cyanol (v/v) and heated at 95 °C for 2 min to ensure reaction quenching. Products were separated on 20% polyacrylamide (w/v)/7 M urea gels by electrophoresis at a constant voltage (2500 V) for 3 h. Radioactive products were then visualized using a phosphorImager, and the bands corresponding to single nucleotide-extended primer were quantified using Quantity One software. For the determination of steady-state kinetic values, graphs of product formation versus dNTP concentration were plotted using nonlinear regression analysis (one-site hyperbolic fits in GraphPad Prism).

Pre-Steady-State Kinetic Analysis. Pre-steady-state experiments were performed using a KinTek RQF-3 model chemical quench-flow apparatus (KinTek Corp., Austin, TX) with 50 mM Na-MOPS (pH 7.5) buffer in the drive syringes. The rapid quench reactions were carried out at 37 °C in the presence of

50 mM MOPS (pH 7.5), 50 mM NaCl, 5 mM DTT, 10 μg/mL BSA, 5% (v/v) glycerol, 50 nM annealed 5′-end-labeled primer-template, 25 nM hPol κ, and 1 mM dCTP. Polymerase catalysis was stopped at different time points by the addition of 500 mM EDTA (pH 9.0). Substrate and product DNA were separated by electrophoresis on a 20% polyacrylamide (w/v)/7 M urea gel. Results obtained under single-turnover conditions were fit to the equation

$$y = A(1 - e^{-k_{obs}t})$$

where A is the product formed in the first extension event, k_{obs} is the rate constant defining polymerization under the conditions used for the experiment being analyzed, and t is time.

LC-MS/MS Analysis. Control and M_1dG-containing 18-mer templates were primed with 13-mer sequences containing uracil. Human Pol κ (core enzyme, 19−526) (5 μM) was preincubated with primer-template DNA (10 μM), and the reaction was initiated by addition of dNTP (1 mM each) and $MgCl_2$ (10 mM) in a final volume of 200 μL. Reactions were allowed to proceed at 37 °C for 5 h in the presence of 50 mM Na-MOPS (pH 7.5) buffer, 50 mM NaCl, 1 mM DTT, 100 μg/mL BSA, and 5% glycerol (v/v). The reaction was terminated by extraction of the remaining dNTPs using a size-exclusion chromatography column (Bio-Spin 6 chromatography column; Bio-Rad). Concentrated stocks of Na-MOPS (pH 7.5), DTT, and EDTA were added to restore the concentrations to 50, 5, and 1 mM, respectively. Later, *E. coli* uracil DNA glycosylase (20 units) was added, and the solution was incubated at 37 °C overnight to hydrolyze the uracil residue on the extended primer. The reaction mixture was then heated at 95 °C for 1 h in the presence of 0.25 M piperidine, followed by removal of the solvent by centrifugation under vacuum. The dried sample was resuspended in 100 μL of H_2O for MS analysis. LC-MS/MS analysis was performed on a Waters Aquity UPLC system (Waters, Milford, MA) connected to a Finnigan LTQ mass spectrometer operating in the ESI negative ion mode, as described previously (*31*, *32*). An estimate for the amount of each product in the reaction mixture was made by integrating the area of the corresponding peak in a selected ion trace for the ion of interest.

RESULTS

Primer Extension Opposite dG and M_1dG by hPol κ. Primer extension studies were performed in order to investigate the ability of hPol κ to synthesize DNA from templates containing a single M_1dG lesion. Templates containing M_1dG at the 19th position from the 3′ end of the template were annealed to ^{32}P-labeled 18-mer primers. The results of *in vitro* synthesis from M_1dG-containing templates are shown in two different sequence contexts, one containing dC and the other containing dT immediately 5′ to the M_1dG residue (Figure 2). Similar results were obtained in both sequence contexts. The extent of synthesis was reduced by the presence of M_1dG in the template, so that product lengths were shorter at each time point when synthesis was catalyzed from M_1dG-containing templates as compared to controls. The shorter bands can result from incomplete extension or deletions. In the present case, the principal source is incomplete extension (see below).

Steady-State Kinetic Analysis of dNTP Insertion Opposite dG and M_1dG by hPol κ. To investigate hPol κ's ability to insert each nucleotide opposite the lesion, experiments were conducted in which control or M_1dG-modified templates were

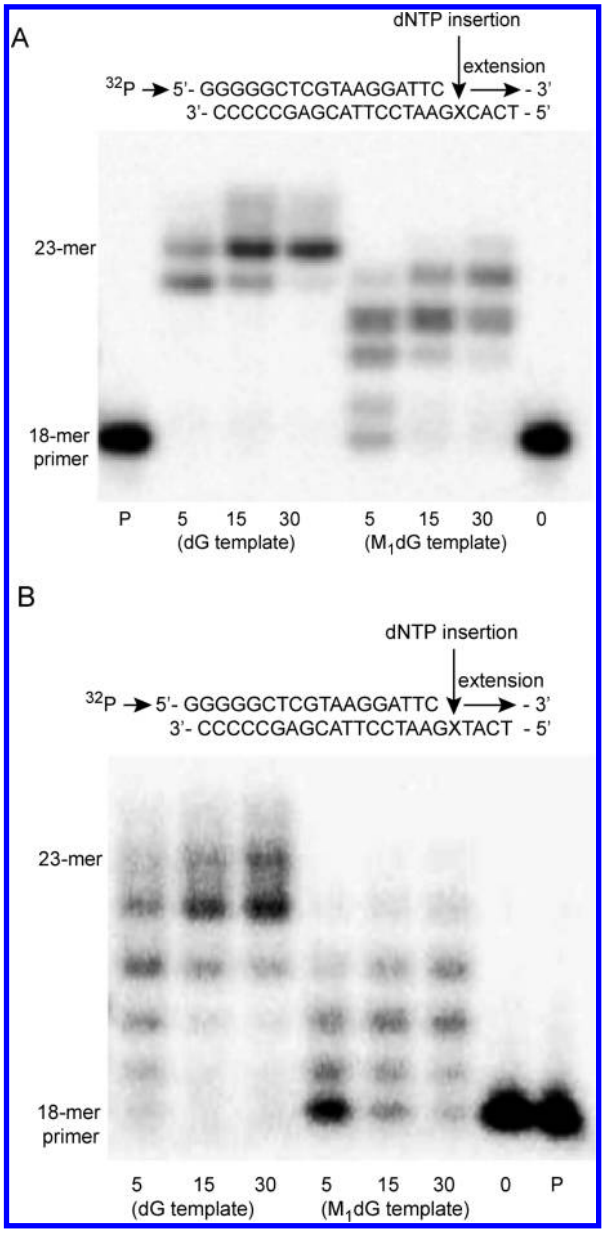

FIGURE 2: Primer extension by hPol κ opposite dG and M_1dG. hPol κ (5 nM) was incubated in the presence of either unmodified or M_1dG-modified 18/23-mer radiolabeled substrate (50 nM) and four dNTPs (500 μM). Template sequences with M_1dG in 3′-GXC-5′ (A) or 3′-GXT-5′ (B) contexts were incubated for the indicated time points at 37 °C. The quenched (EDTA) samples were analyzed by 20% (w/v) denaturing polyacrylamide gel electrophoresis, and the amount of product formation was visualized using a phosphorimaging device. P represents the migration of the starting primer.

incubated with the enzyme and single dNTPs (Figure 3). All four dNTPs were incorporated in control and M_1dG-containing DNA in both sequence contexts. Differences were observed in the migration of some of the products between unadducted and adducted templates as a result of the incorporation of different numbers of dNTPs.

The results in Figure 3 suggested that hPol κ's nucleotide insertion efficiency is different opposite M_1dG as opposed to dG. Consequently, steady-state kinetic reactions were performed in order to quantify the single nucleotide preference of hPol κ during insertion opposite M_1dG in both sequence contexts (Table 2). The specificity constant (k_{cat}/K_m) provides a measure of the catalytic efficiency for each dNTP insertion reaction and allows

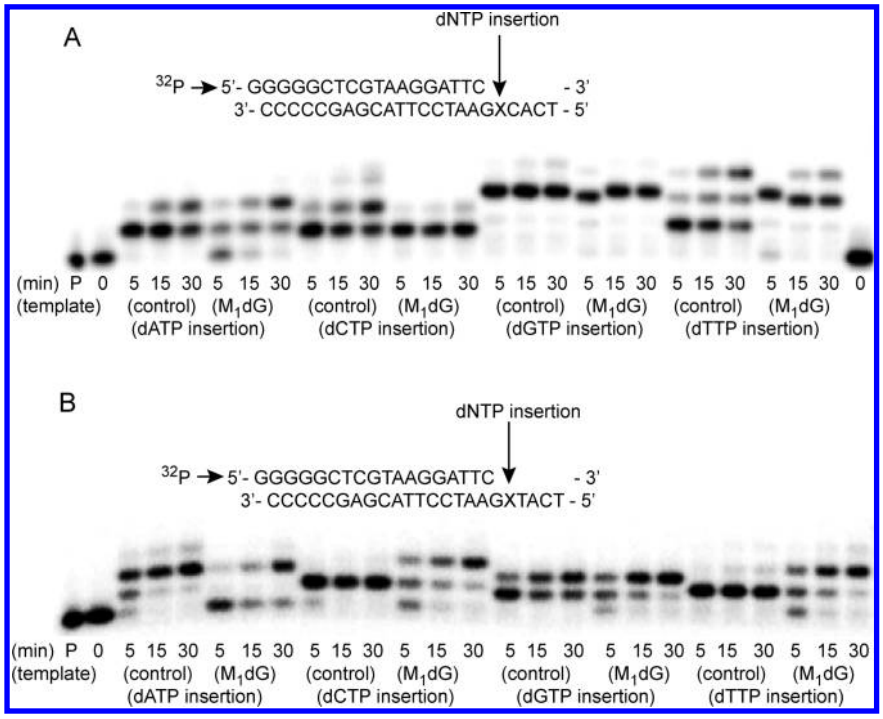

FIGURE 3: Single nucleotide insertion by hPol κ opposite dG and M_1dG. hPol κ (5 nM) was incubated in the presence of either unmodified or M_1dG-modified 18/23-mer radiolabeled substrate (50 nM) and a single dNTP (500 μM) as indicated. Template sequences with M_1dG in 3′-GXC-5′ (A) or 3′-GXT-5′ (B) contexts were incubated for the indicated time points at 37 °C. The quenched (EDTA) samples were analyzed by 20% (w/v) denaturing polyacrylamide gel electrophoresis, and the amount of product formation was visualized using a phosphorimaging device. P represents the migration of the starting primer.

Table 2: Steady-State Kinetic Parameters for Single Nucleotide Insertion by hPol κ Opposite dG and M_1dG[a]

	DNA substrate	incoming nucleotide	k_{cat} (min^{-1})	K_m(dNTP) (μM)	k_{cat}/K_m (μM^{-1} min^{-1})	f (relative insertion frequency)
Part A	insertion opposite dG					
	5′-TTC	dCTP	4.1 ± 0.4	1.9 ± 1	2.1	1
	3′-AAGXCACT-5′	dATP	0.2 ± 0.01	22 ± 8	0.009	0.004
	X = dG	dGTP	1.3 ± 0.1	56 ± 29	0.02	0.009
		dTTP	1.6 ± 0.2	61 ± 36	0.02	0.009
	insertion opposite M_1dG					
	5′-TTC	dCTP	1.3 ± 0.1	19 ± 9	0.068	0.03
	3′-AAGXCACT-5′	dATP	0.07 ± 0.007	12 ± 6	0.005	0.002
	X = M_1dG	dGTP	0.1 ± 0.006	10 ± 3	0.01	0.004
		dTTP	0.07 ± 0.005	5 ± 2	0.014	0.006
Part B	insertion opposite dG					
	5′-TTC	dCTP	3 ± 0.2	1.3 ± 0.6	2.3	1
	3′-AAGXTACT-5′	dATP	0.1 ± 0.01	5 ± 3	0.02	0.008
	X = dG	dGTP	1.4 ± 0.1	32 ± 20	0.02	0.008
		dTTP	1.4 ± 0.2	36 ± 23	0.03	0.01
	insertion opposite M_1dG					
	5′-TTC	dCTP	0.6 ± 0.09	6 ± 4	0.1	0.04
	3′-AAGXTACT-5′	dATP	0.03 ± 0.004	2 ± 1	0.01	0.004
	X = M_1dG	dGTP	0.09 ± 0.005	10 ± 3	0.01	0.004
		dTTP	0.08 ± 0.002	13 ± 2	0.006	0.002

[a]For determination of steady-state kinetic values, graphs of product formation versus dNTP concentration were analyzed using nonlinear regression (one-site hyperbolic fit) in the GraphPad Prism program. The relative insertion frequencies were calculated relative to insertion of dCTP opposite control (dG) primer-templates as the ratio $(k_{cat}/K_m)_{dNTP}/(k_{cat}/K_m)_{dCTP}$.

comparisons to be made between dNTP insertion events. Kinetic analysis of the hPol κ-catalyzed insertion of dCMP opposite dG yielded K_m and k_{cat} values comparable to those reported previously (*33*). The insertion of dCMP opposite M_1dG was the most favored reaction for the 3′-GXC-5′ template and was 33-fold less efficient than insertion of dCMP opposite dG (Table 2). A similar result was obtained using the 3′-GXT-5′ template, in which incorporation of dCMP opposite M_1dG was 25-fold less efficient than incorporation of dCMP opposite dG. hPol κ inserted dTMP, dGMP, and dAMP opposite the M_1dG lesion 5-, 7.5-, and 15-fold less efficiently than dCMP incorporation opposite the lesion in the 3′-GXC-5′ context. Similar

catalytic efficiencies were observed with the 3′-GXT-5′ template although the incorporation of dGMP was slightly greater than the incorporation of dTMP. As observed with the 3′-GXC-5′ template, incorporation of dAMP was slowest. These results suggest that hPol κ preferentially incorporates dCMP opposite M_1dG *in vitro* in both sequence contexts and that other dNMPs are incorporated at somewhat reduced rates.

Pre-Steady-State Kinetic Analysis of dCMP Insertion Opposite dG and M_1dG by hPol κ. Transient-state kinetic analysis was used to further assess the catalytic properties of hPol κ in bypassing the M_1dG lesion. Template-primers (50 nM) were combined with 25 nM hPol κ and then mixed with an excess of dCTP. The reaction was quenched after different reaction times. The time course of dCMP incorporation in experiments with an unadducted template displayed typical burst kinetics and indicated that 100% of the enzyme molecules were bound to template/primer in a productive manner when dCTP was added to the reaction mixture (Figure 4). The observed rate (k_{obs}) in the control reaction was very similar to the maximum forward rate of polymerization (k_{pol}) reported elsewhere (*29*). dCMP incorporation from adducted templates was significantly inhibited compared to the unadducted templates. The amplitude of product formation decreased roughly 90%, and the observed rate constant for dCMP insertion opposite M_1dG decreased 43-fold (Figure 4). Thus, the transient-state kinetic results are consistent with results obtained in the steady-state kinetic experiments, demonstrating M_1dG significantly reduces the efficiency of replication by hPol κ.

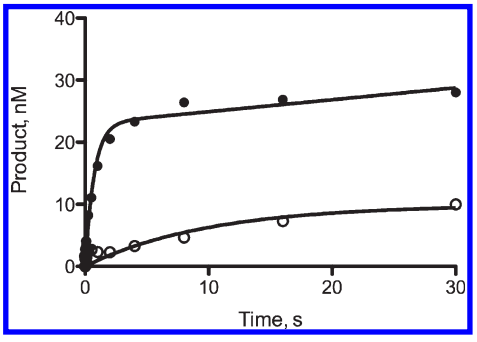

FIGURE 4: Pre-steady-state kinetics of dCTP insertion by hPol κ opposite dG and M_1dG. Kinetic analysis was performed using 50 nM 18/23-mer ^{32}P-labeled substrate and 25 nM enzyme. Reactions were initiated by rapid addition of a 1 mM dCTP and 10 nM $MgCl_2$ solution to preincubated enzyme primer-template mix and quenched by the addition of EDTA after varying times ranging from 0.01 to 30 s.

Kinetic Parameters of Next-Base Extension from Matched and Mismatched Primer Termini by hPol κ. A key determinant of the outcome of replication is the rate at which primers containing different dNMPs opposite M_1dG are extended. We performed next-base extension studies by using primers containing different dNMPs opposite either dG or M_1dG in the template strand. Only template-primers containing the 3′-GXC-5′ sequence were used for these studies; the various template-primers containing different primer termini were incubated with hPol κ and dGTP (Table 3). As expected, dGMP incorporation was most efficient when the primer terminus contained dC opposite dG in the template. The rates of extension of a mismatched dN primer-dG template were significantly reduced. The rates of extension of primer-templates containing various dNMPs opposite M_1dG were also significantly reduced compared to the extension of the dC primer-dG template. However, the rate of extension of the dC primer-M_1dG template was greater than the rates of extension of the other mismatched dN:M_1dG primer-template termini. In order to probe for the potential for extension of slipped mispairs at the primer-template termini, the rates of extension of dG:dG and dG:M_1dG by incorporation of dTMP were determined. The rates were comparable to those measured for the incorporation of dGMP from either primer-template. The rate of extension of dG:M_1dG was somewhat greater than dG:dG. Thus, mispairing may contribute to the production of the incomplete extension products observed in Figure 2.

Primer Extension and dNTP Insertion Opposite dG and M_1dG by hPol ι and Rev1. The primer extension experiments described above for hPol κ were also conducted with hPol ι and Rev1 (ratio of template-primer:enzyme of 10:1). The results revealed that both hPol ι and Rev1 inserted dNMPs opposite M_1dG but did not extend beyond the insertion site (Figure 5). The identity of the deoxynucleotides inserted was probed with single nucleotide incorporation experiments (Tables 4 and 5). hPol ι inserted dCMP or dTMP opposite M_1dG most efficiently. Steady-state kinetic analysis (Table 4) indicated that hPol ι inserted dCMP opposite M_1dG approximately 7-fold or 21-fold less efficiently than opposite dG: k_{cat}/K_m values for dCMP incorporation opposite M_1dG were 0.1 and 0.08 μM^{-1} min^{-1} in the 3′-GXC-5′ and 3′-GXT-5′ template sequence contexts, respectively. The insertion of dCMP opposite M_1dG by Rev1 was about half as efficient as the insertion of dCMP opposite dG (Table 5).

LC-MS Analysis of hPol κ Catalysis with Unmodified Template DNA. Hpol κ full-length extension products with an

Table 3: Kinetic Parameters for Single Nucleotide Extension by hPol κ of Template-Primers Containing Different Primer-Termini Opposite dG and M_1dG[a]

incoming nucleotide	DNA substrate	k_{cat} (min^{-1})	K_m(dNTP) (μM)	k_{cat}/K_m (μM^{-1} min^{-1})	f (relative insertion frequency)
dGTP	dG:C	4.6 ± 0.1	0.8 ± 0.02	5.7	1
	dG:A	0.3 ± 0.02	16 ± 6	0.01	0.001
	dG:G	1.0 ± 0.1	32 ± 16	0.03	0.005
	dG:T	0.1 ± 0.005	3.4 ± 1	0.02	0.003
dGTP	M_1dG:C	0.7 ± 0.2	1.4 ± 0.3	0.5	0.08
	M_1dG:A	0.1 ± 0.07	2.5 ± 0.8	0.04	0.007
	M_1dG:G	0.3 ± 0.01	4.0 ± 1.0	0.07	0.01
	M_1dG:T	0.2 ± 0.01	3.8 ± 1.4	0.05	0.008
dTTP	dG:G	1.2 ± 0.1	42 ± 18	0.02	0.003
	M_1dG:G	0.2 ± 0.008	2.4 ± 0.5	0.08	0.01

[a]One-base extension experiments were conducted using a template-primer with the 3′-GXC-5′ sequence in the template and the base pair listed as substrate for X:N. Kinetic parameters were determined as described in Table 2.

unmodified DNA substrate were analyzed by LC-MS in order to establish the level of background misinsertion events detected by this method. Deoxyuridine was placed in the penultimate position of the primer, which enabled uracil DNA glycosylase to be used to remove the 5′ end of the primer. The oligonucleotide

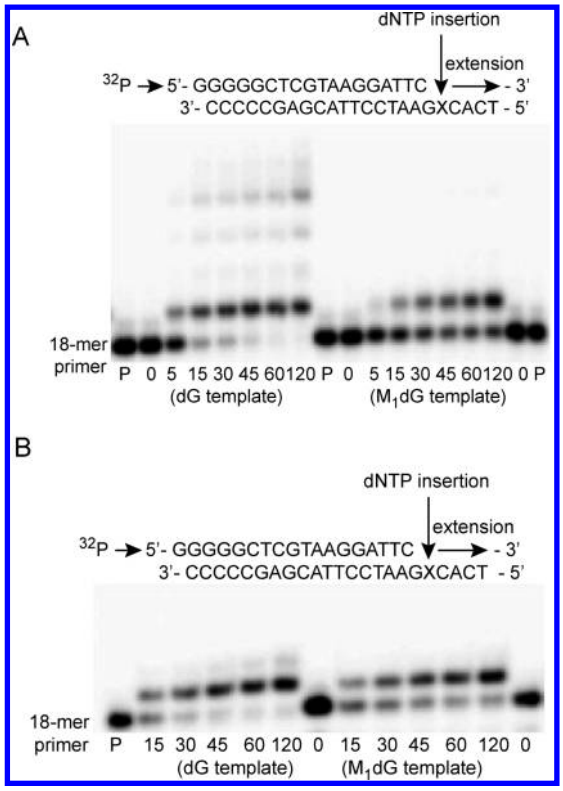

FIGURE 5: Primer extension by hPol ι and Rev1 opposite dG and M_1dG. hPol ι or Rev1 (5 nM) was incubated in the presence of either unmodified or M_1dG-modified 18/23-mer ^{32}P-labeled substrate (50 nM) and four dNTPs (500 μM). The template containing 3′-G-(M_1dG)C-5′ is shown, along with the results for hPol ι (A) and Rev 1 (B). Incubations were conducted for different times at 37 °C. The quenched (EDTA) samples were analyzed by 20% (w/v) denaturing polyacrylamide gel electrophoresis, and the amount of product formation was visualized using a phosphorimaging device. P represents the migration of the starting primer.

products were analyzed by LC-MS/MS as described elsewhere (*31*, *32*). Two major product ions were identified in the spectra (Figure 6). Both represented accurate copying of the template strand. The first (m/z = 1087, M_1 − 2H) was determined to be correct insertion of dCTP opposite dG, followed by accurate full-length extension. The second ion (m/z = 930, M_2 − 2H) was identified as an accurate copying event that terminates one base short of the 5′-terminus of the template DNA.

LC-MS/MS Analysis of Fully Extended hPol κ DNA Products Synthesized on a Template Containing a Single M_1dG. Parallel reactions were conducted with templates containing M_1dG in the 3′-GXC-5′ or 3′GXT-5′ sequence. The molecular ions of the major products of replication past M_1dG in the 3′-GXC-5′ (A, B, and C) and 3′-GXT-5′ (D, E, and F) contexts, as well as the identities of the products and their relative abundances are shown in Figure 7. The major products in both contexts resulted from insertion of dCMP opposite the M_1dG residue, as anticipated from the results of the single nucleotide insertion experiments. In the 3′-GXC-5′ context, other products resulted from insertion of dAMP or dTMP opposite M_1dG and a one-base deletion in which dGMP was inserted opposite the template dC immediately 5′ to M_1dG. Interestingly, some products appeared to result from insertion of TGG or ACG opposite the template, XC, which potentially led to misinsertion and a one-base addition. In the 3′-GXT-5′ context, the only products resulted from dCMP or dAMP insertion. A small amount of a one-base deletion product was observed in which dAMP was inserted opposite template dT, immediately 5′ to M_1dG, but the major products resulting from dAMP incorporation also displayed mispaired sequences beyond the initial insertion point. Some truncated extension products were observed in both sequence contexts regardless of the identity of the base inserted opposite M_1dG.

DISCUSSION

The present results demonstrate that hPol κ, hPol ι, and Rev1 are able to insert deoxynucleotides opposite M_1dG and that hPol κ is able to extend template-primers containing deoxynucleotides opposite the lesion. All three enzymes preferentially inserted dCMP opposite M_1dG but the efficiency of insertion of dCMP by

Table 4: Steady-State Kinetic Parameters for Single Nucleotide Insertion by hPol ι Opposite dG and M_1dG[a]

	DNA substrate	incoming nucleotide	k_{cat} (min^{-1})	K_m(dNTP) (μM)	k_{cat}/K_m (μM^{-1} min^{-1})	f (relative insertion frequency)
Part A	insertion opposite dG					
	5′-TTC	dCTP	0.35 ± 0.05	3.4 ± 2.0	0.1	1
	3′-AAGXCACT-5′	dTTP	0.10 ± 0.005	16 ± 4	6×10^{-3}	0.06
	X = dG					
	insertion opposite M_1dG					
	5′-TTC	dCTP	0.34 ± 0.003	2.4 ± 1	0.014	0.14
	3′-AAGXCACT-5′	dTTP	0.028 ± 0.003	24 ± 14	1×10^{-3}	0.01
	X = M_1dG					
Part B	insertion opposite dG					
	5′-TTC	dCTP	0.73 ± 0.03	8.4 ± 2.3	0.087	1
	3′-AAGXTACT-5′	dTTP	0.40 ± 0.04	3.6 ± 1.9	0.1	1.1
	X = dG					
	insertion opposite M_1dG					
	5′-TTC	dCTP	0.04 ± 0.005	9.4 ± 6	4.2×10^{-3}	0.04
	3′-AAGXTACT-5′	dTTP	0.17 ± 0.020	27 ± 16	6.2×10^{-3}	0.07
	X = M_1dG					

[a]Kinetic parameters were determined as described in Table 2.

Table 5: Steady-State Kinetic Parameters for Single Nucleotide Insertion by Rev1 Opposite dG and M_1dG[a]

	DNA substrate	incoming nucleotide	k_{cat} (min^{-1})	K_m(dNTP) (μM)	k_{cat}/K_m (μM^{-1} min^{-1})	f (relative insertion frequency)
Part A	insertion opposite dG					
	5′-TTC 3′-AAGXCACT-5′ X = dG	dCTP	1.5 ± 0.2	61 ± 35	0.02	1
	insertion opposite M_1dG					
	5′-TTC 3′-AAGXCACT-5′ X = M_1dG	dCTP	0.6 ± 0.09	42 ± 33	0.01	0.5
Part B	insertion opposite dG					
	5′-TTC 3′-AAGXTACT-5′ X = dG	dCTP	1.3 ± 0.1	92 ± 40	0.01	1
	insertion opposite M_1dG					
	5′-TTC 3′-AAGXTACT-5′ X = M_1dG	dCTP	0.6 ± 0.04	88 ± 25	6.8×10^{-3}	0.6

[a]Kinetic parameters were determined as described in Table 2.

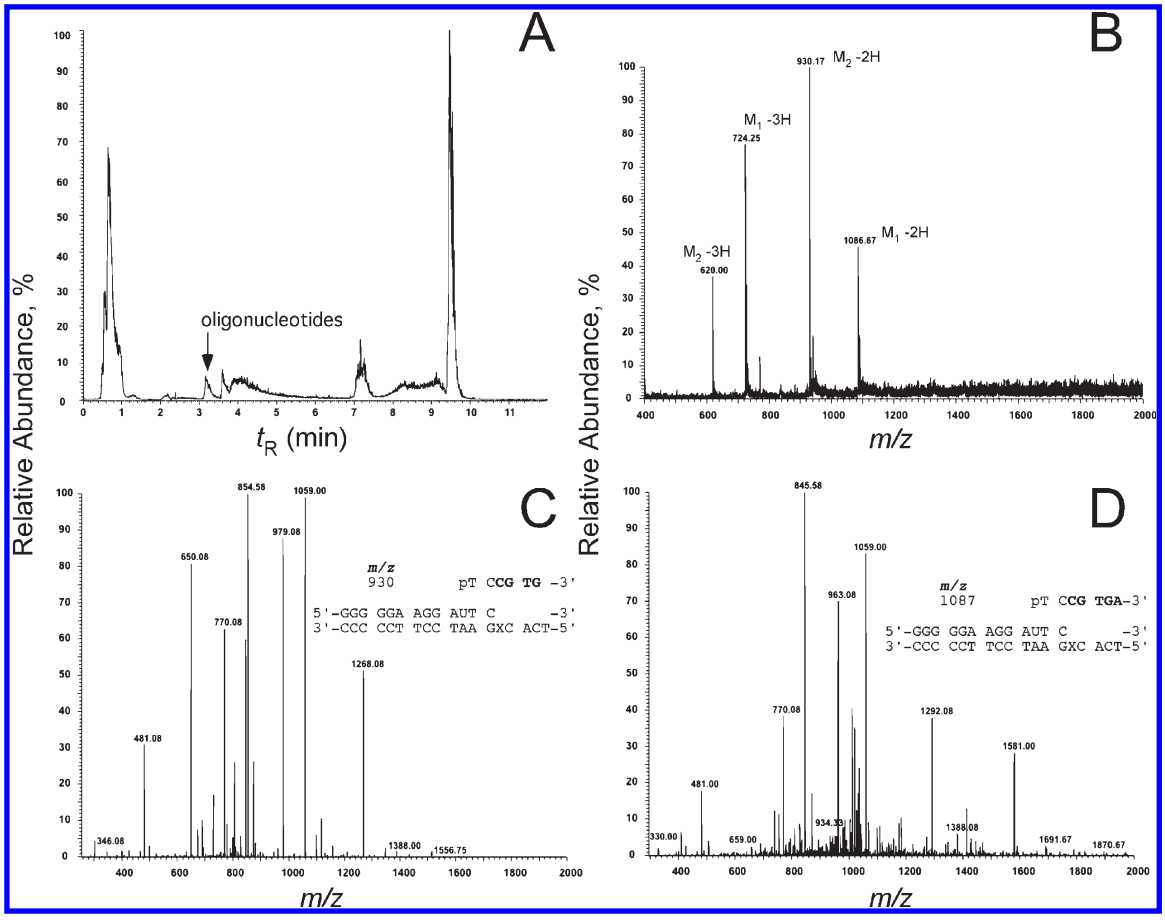

FIGURE 6: LC-MS analysis of hPol κ-catalyzed *in vitro* replication products on unmodified DNA. Oligonucleotides eluting at t_R = 3.2 min (A) were analyzed by mass spectrometry (B). Doubly and triply charged ions were detected for two products. The mass spectra and sequences of the doubly charged ions at m/z = 930 and 1087 are depicted in (C) and (D), respectively.

Rev1 and hPol ι was approximately 15- and 4-fold higher than the insertion of dCMP by hPol κ, respectively. hPol ι inserted dTMP 13−16-fold less efficiently than dCMP (depending on sequence context) and inserted purine deoxynucleosides very poorly. In contrast, hPol κ inserted dTMP, dGMP, and dAMP at comparable rates, which are 5−10-fold lower than the rate of incorporation of dCMP. Single nucleotide incorporation experiments indicate that hPol κ extended template-primers containing dC opposite M_1dG approximately 10-fold more efficiently than template-primers containing other deoxynucleotides opposite the adduct when it is contained in the 3′-GXC-5′ sequence. The product of the rates of hPol κ-catalyzed insertion of dCMP opposite M_1dG and one-base extension past dC-M_1dG was 400-fold lower than the product of the same rates for hPol κ

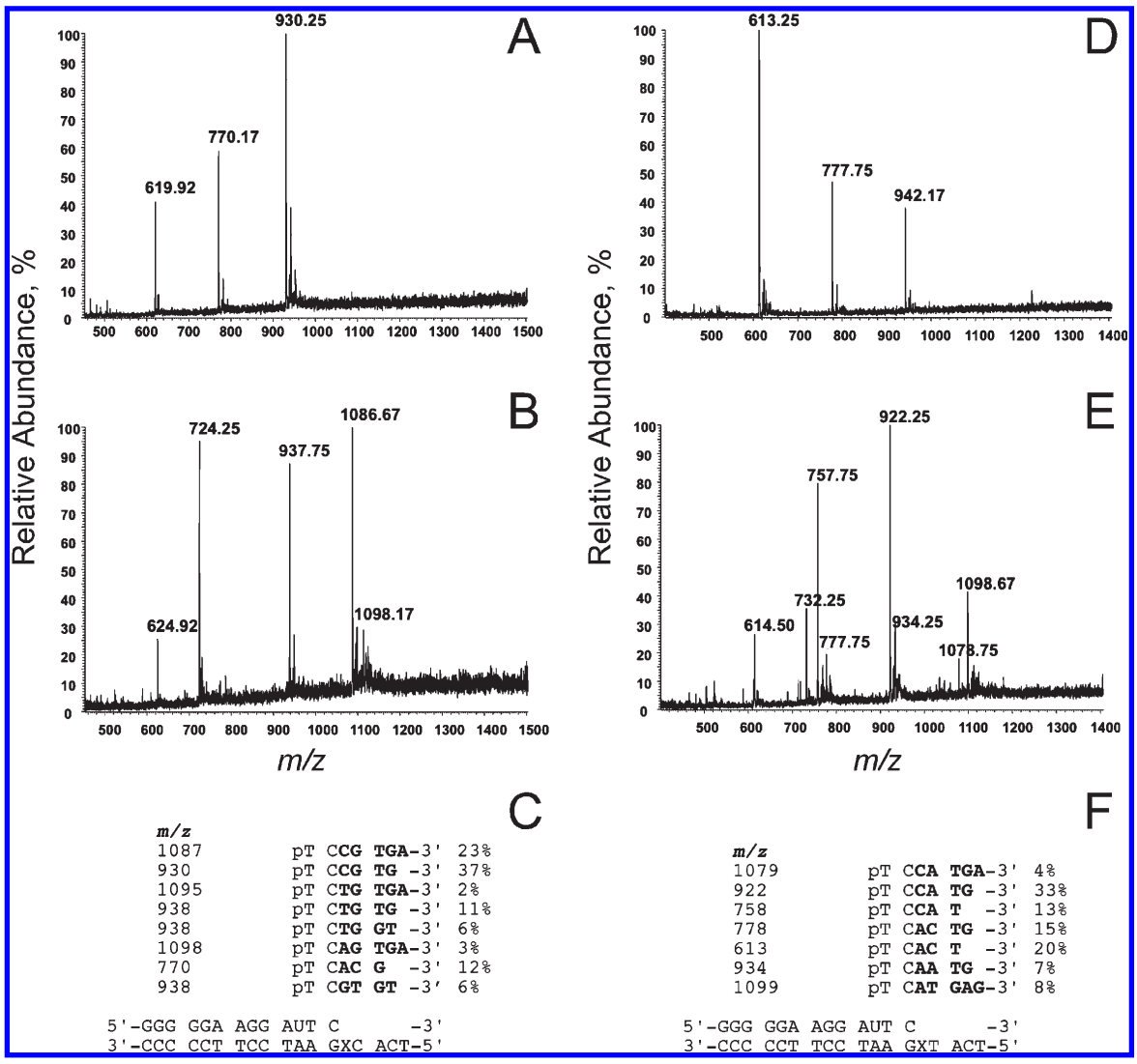

FIGURE 7: LC-MS analysis of hPol κ-catalyzed *in vitro* replication products of the bypass of M_1dG-modified DNA. The mass spectra for product ions eluting at (A) t_R = 2.0−2.3 min and (B) t_R = 2.9−3.2 min are shown for hPol κ-catalyzed bypass of M_1dG-containing template DNA with the 3′-GXC-5′ sequence. (C) The resulting products identified by CID fragmentation patterns are shown in schematic form. The mass spectra for product ions eluting at (D) t_R = 2.6−2.8 min and (E) t_R = 2.9−3.2 min are shown for hPol κ-catalyzed bypass of M_1dG-containing template DNA with the 3′-G(M_1dG)T-5′ sequence. (F) Products identified by CID fragmentation patterns are shown in schematic form.

acting on unmodified template-primers (1/0.03 × 0.08). So although hPol κ is capable of bypassing M_1dG lesions, it is much less efficient than when it is acting on unmodified templates.

LC/MS analyses of the products of hPol κ-catalyzed extension of template-primers containing M_1dG indicate that dCMP was incorporated opposite the lesion in 50% of the products, regardless of whether the sequence of the template was 3′-GXC-5′ or 3′-GXT-5′. The remaining products arose from roughly equal incorporation of dTMP or dAMP opposite M_1dG in the 3′-GXC-5′ context or exclusively dAMP in the 3′GXT-5′ context. Analysis of bypass products captures the outcome of both insertion and extensions so some differences from the results of individual insertion and extension experiments are anticipated. For example, bypass product analysis in the 3′-GXT-5′ sequence context revealed that insertion of dAMP opposite the lesion accounted for one-half of the products, a finding that would not have been predicted from the results of the single nucleotide insertion experiments alone. Because a dT residue was positioned 5′ to the lesion, slippage or misalignment might have occurred to enable lesion bypass to generate deletion products. Such deletion products were detected by mass spectrometry and were expected based on detection of truncated products from ^{32}P-labeled template-primers by polyacrylamide gel electrophoresis (Figure 2). However, it is noteworthy that most of the truncated oligonucleotide products were incomplete extension products rather than nucleotide deletion products.

The present results are reminiscent of the results of hPol κ and hPol ι bypass of the exocyclic adducts propanodeoxyguanosine (PdG), γ-hydroxy-PdG, and the alkyl-substituted γ-hydroxy-PdG adducts derived from reaction of 4-hydroxynonenal with dG (*26*−*28*). In all cases, hPol ι incorporated dCMP opposite the lesion nearly as efficiently as it incorporated dCMP opposite dG, but hPol ι did not extend past the lesion. Human Pol ι also incorporates dTMP opposite the exocyclic lesions but less efficiently than dCMP. Human Pol κ inserted dCMP opposite the exocyclic lesions less efficiently than hPol ι did, but hPol κ was able to extend template-primers containing dNMPs opposite the adducts. These observations led to the hypothesis that hPol ι and hPol κ collaborate to effect bypass such that hPol ι catalyzes insertion and hPol κ catalyzes extension (*26*). A similar hypothesis could be advanced to include Rev1, along with hPol ι and hPol κ, on the basis of the present experiments, although multiple

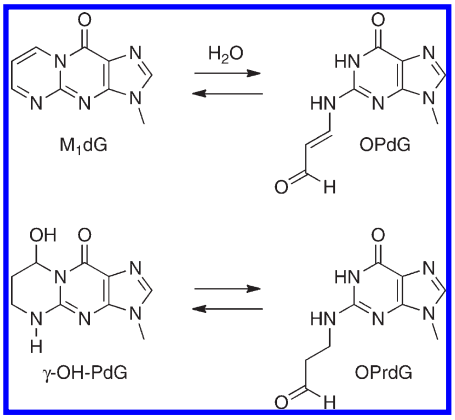

FIGURE 8: M_1dG and γ-OH-PdG ring opening.

factors will affect bypass at the replication fork (e.g., the amounts of the various bypass polymerases in a cell, relative catalytic activities, and their propensity for interaction with ancillary replication machinery, such as PCNA).

A significant difference exists in the hPol κ-catalyzed extension of template-primers containing dC opposite M_1dG as compared to γ-hydroxy-PdG. hPol κ catalyzes extension of the dC:M_1dG mismatch approximately 12.5-fold less efficiently than it catalyzed the extension of a dC:dG match (Table 3). In contrast, hPol κ catalyzes extension of the dC:γ-hydroxy-PdG mismatch 3.3-fold more efficiently than it catalyzes extension of a dC:dG match (*26*). This dramatic difference in extension kinetics is proposed to be due to the relative propensities of M_1dG and γ-hydroxy-PdG to ring-open in the active site of a polymerase. Both adducts ring-open in duplex DNA when placed opposite dC residues (*13*, *34*); neither adduct ring-opens when placed opposite dT residues in duplex DNA. M_1dG opens to 2-(3-oxopropenyl)-dG whereas γ-hydroxy-PdG opens to 2-(3-oxopropyl)-dG (Figure 8). Both ring-opened adducts lie in the minor groove and do not prevent Watson−Crick base pairing between the adducted dG and the dC opposite it. Thus, the ring-opened adducts are more easily bypassed and are less miscoding than the ring-closed adducts. The high efficiency of Pol κ-catalyzed extension of template-primers containing dC opposite γ-hydroxy-PdG has been proposed to reflect extension of the hydrogen-bonded dC:2-(3-oxopropyl)-dG base pair (*26*). Support for this hypothesis is provided by the observation that hPol κ is very inefficient at extending template-primers containing dC:PdG termini (*27*). In contrast to γ-hydroxy-PdG, PdG is chemically stable in duplex DNA and does not ring-open.

The prior results of extension of dC:γ-hydroxy-PdG-containing template-primers by hPol κ imply that the dC:2-(3-oxopropyl)-dG base pair binds to hPol κ or that ring opening occurs in the active site. The low efficiency of extension of dC:M_1dG-containing template-primers by hPol κ suggests that the adduct remains ring-closed, both in solution and in the hPol κ active site. The latter conclusion is consistent with recent work from our laboratory, which reported the structure of a template-primer containing a dC-M_1dG terminus bound in the active site of the archeal Y-family polymerase, Dpo4 (*25*). The M_1dG adduct was present in the Dpo4 active site in the ring-closed form, and the dC residue was rotated out of the active site and lay in the minor groove. Although this configuration is not productive from the standpoint of extension, its existence implies that a dC:2-(3-oxopropenyl)-dG base pair does not form or is not stable in the active site of a Y-family polymerase. In fact, it may also provide insights into why the extension of dC:M_1dG template-primers is so slow, because the dC residue must rotate to a position where its 3′-hydroxyl group can attack the α-phosphoryl group of an incoming dNTP.

The present results, taken with prior studies of hPol η, provide a comprehensive picture of bypass of M_1dG lesions by Y-family DNA polymerases. The kinetics of insertion and extension by hPol η, hPol κ, hPol ι, and Rev1, as well as the identity of the products formed, have been determined for M_1dG residues contained in the same template-primer sequence. To a first approximation, it appears that hPol η is responsible for incorporation of dAMP opposite M_1dG while Rev1, hPol ι, and hPol κ are responsible for incorporation of dCMP and dTMP. Both hPol η and hPol κ introduce frameshift mutations at the site of the adduct. These events correlate to the spectrum of mutations induced by M_1dG on a shuttle vector replicated in COS-7 monkey kidney cells (*16*). Mutations were induced at a frequency of 2%, and $M_1dG \rightarrow T$ predominated over $M_1dG \rightarrow A$; frameshifts occurred but only when the lesion was located in a reiterated sequence context. We propose that $M_1dG \rightarrow T$ mutations are introduced by hPol η and $M_1dG \rightarrow A$ mutations are introduced by a combination of hPol ι and hPol κ. Frameshift mutations can be introduced by either hPol η or hPol κ. Interestingly, non-targeted mutations were observed at sites near but past the lesion site (*16*). This type of nontargeted mutation is observed with hPol κ but not hPol η (Figure 6). It will interesting to evaluate the importance of individual Y-family polymerases in M_1dG bypass in intact cells to determine if the results of *in vitro* experiments can be extrapolated to more complex cellular systems.

REFERENCES

1. Marnett, L. J., and Plastaras, J. P. (2001) Endogenous DNA damage and mutation. *Trends Genet. 17*, 214–221.
2. Migliore, L., and Coppede, F. (2002) Genetic and environmental factors in cancer and neurodegenerative diseases. *Mutat. Res. 512*, 135–153.
3. Olinski, R., Gackowski, D., Foksinski, M., Rozalski, R., Roszkowski, K., and Jaruga, P. (2002) Oxidative DNA damage: assessment of the role in carcinogenesis, atherosclerosis, and acquired immunodeficiency syndrome. *Free Radical Biol. Med. 33*, 192–200.
4. Marnett, L. J. (1999) Lipid peroxidation-DNA damage by malondialdehyde. *Mutat. Res. 424*, 83–95.
5. Dedon, P. C. (2008) The chemical toxicology of 2-deoxyribose oxidation in DNA. *Chem. Res. Toxicol. 21*, 206–219.
6. Basu, A. K., O'Hara, S. M., Valladier, P., Stone, K., Mols, O., and Marnett, L. J. (1988) Identification of adducts formed by reaction of guanine nucleosides with malondialdehyde and structurally related aldehydes. *Chem. Res. Toxicol. 1*, 53–59.
7. Dedon, P. C., Plastaras, J. P., Rouzer, C. A., and Marnett, L. J. (1998) Indirect mutagenesis by oxidative DNA damage: formation of the pyrimidopurinone adduct of deoxyguanosine by base propenal. *Proc. Natl. Acad. Sci. U.S.A. 95*, 11113–11116.
8. Zhou, X., Taghizadeh, K., and Dedon, P. C. (2005) Chemical and biological evidence for base propenals as the major source of the endogenous M_1dG adduct in cellular DNA. *J. Biol. Chem. 280*, 25377–25382.
9. Chaudhary, A. K., Nokubo, M., Reddy, G. R., Yeola, S. N., Morrow, J. D., Blair, I. A., and Marnett, L. J. (1994) Detection of endogenous malondialdehyde-deoxyguanosine adducts in human liver. *Science 265*, 1580–1582.
10. Jeong, Y. C., Sangaiah, R., Nakamura, J., Pachkowski, B. F., Ranasinghe, A., Gold, A., Ball, L. M., and Swenberg, J. A. (2005) Analysis of M_1G-dR in DNA by aldehyde reactive probe labeling and liquid chromatography tandem mass spectrometry. *Chem. Res. Toxicol. 18*, 51–60.
11. Jeong, Y. C., Nakamura, J., Upton, P. B., and Swenberg, J. A. (2005) Pyrimido[1,2-a]-purin-10(3H)-one, M_1G, is less prone to artifact than base oxidation. *Nucleic Acids Res. 33*, 6426–6434.
12. Jeong, Y. C., Walker, N. J., Burgin, D. E., Kissling, G., Gupta, M., Kupper, L., Birnbaum, L. S., and Swenberg, J. A. (2008) Accumulation

of M_1dG DNA adducts after chronic exposure to PCBs, but not from acute exposure to polychlorinated aromatic hydrocarbons. *Free Radical Biol. Med. 45*, 585–591.
13. Mao, H., Schnetz-Boutaud, N. C., Weisenseel, J. P., Marnett, L. J., and Stone, M. P. (1999) Duplex DNA catalyzes the chemical rearrangement of a malondialdehyde deoxyguanosine adduct. *Proc. Natl. Acad. Sci. U.S.A. 96*, 6615–6620.
14. Riggins, J. N., Daniels, J. S., Rouzer, C. A., and Marnett, L. J. (2004) Kinetic and thermodynamic analysis of the hydrolytic ring-opening of the malondialdehyde-deoxyguanosine adduct, 3-(2′-deoxy-beta-D-erythro-pentofuranosyl)- pyrimido[1,2-alpha]purin-10(3H)-one. *J. Am. Chem. Soc. 126*, 8237–8243.
15. Fink, S. P., Reddy, G. R., and Marnett, L. J. (1997) Mutagenicity in *Escherichia coli* of the major DNA adduct derived from the endogenous mutagen malondialdehyde. *Proc. Natl. Acad. Sci. U.S.A. 94*, 8652–8657.
16. VanderVeen, L. A., Hashim, M. F., Shyr, Y., and Marnett, L. J. (2003) Induction of frameshift and base pair substitution mutations by the major DNA adduct of the endogenous carcinogen malondialdehyde. *Proc. Natl. Acad. Sci. U.S.A. 100*, 14247–14252.
17. Woodgate, R. (1999) A plethora of lesion-replicating DNA polymerases. *Genes Dev. 13*, 2191–2195.
18. Ohmori, H., Friedberg, E. C., Fuchs, R. P., Goodman, M. F., Hanaoka, F., Hinkle, D., Kunkel, T. A., Lawrence, C. W., Livneh, Z., Nohmi, T., Prakash, L., Prakash, S., Todo, T., Walker, G. C., Wang, Z., and Woodgate, R. (2001) The Y-family of DNA polymerases. *Mol. Cell 8*, 7–8.
19. Wang, H., Kozekov, I. D., Kozekova, A., Tamura, P. J., Marnett, L. J., Harris, T. M., and Rizzo, C. J. (2006) Site-specific synthesis of oligonucleotides containing malondialdehyde adducts of deoxyguanosine and deoxyadenosine via a postsynthetic modification strategy. *Chem. Res. Toxicol. 19*, 1467–1474.
20. Lehmann, A. R. (2002) Replication of damaged DNA in mammalian cells: new solutions to an old problem. *Mutat. Res. 509*, 23–34.
21. Prakash, S., Johnson, R. E., and Prakash, L. (2005) Eukaryotic translesion synthesis DNA polymerases: specificity of structure and function. *Annu. Rev. Biochem. 74*, 317–353.
22. Burgers, P. M., Koonin, E. V., Bruford, E., Blanco, L., Burtis, K. C., Christman, M. F., Copeland, W. C., Friedberg, E. C., Hanaoka, F., Hinkle, D. C., Lawrence, C. W., Nakanishi, M., Ohmori, H., Prakash, L., Prakash, S., Reynaud, C. A., Sugino, A., Todo, T., Wang, Z., Weill, J. C., and Woodgate, R. (2001) Eukaryotic DNA polymerases: proposal for a revised nomenclature. *J. Biol. Chem. 276*, 43487–43490.
23. Nelson, J. R., Lawrence, C. W., and Hinkle, D. C. (1996) Thymine-thymine dimer bypass by yeast DNA polymerase zeta. *Science 272*, 1646–1649.
24. Stafford, J. B., Eoff, R. L., Kozekova, A., Rizzo, C. J., Guengerich, F. P., and Marnett, L. J. (2009) Translesion DNA synthesis by human DNA polymerase eta on templates containing a pyrimidopurinone deoxyguanosine adduct, 3-(2′-deoxy-beta-D-erythro-pentofuranosyl)-pyrimido-[1,2-a]purin-10(3H)-one. *Biochemistry 48*, 471–480.
25. Eoff, R. L., Stafford, J. B., Szekely, J., Rizzo, C. J., Egli, M., Guengerich, F. P., and Marnett, L. J. (2009) Structural and functional analysis of *Sulfolobus solfataricus* Y-family DNA polymerase Dpo4-catalyzed bypass of the malondialdehyde-deoxyguanosine adduct. *Biochemistry 48*, 7079–7088.
26. Washington, M. T., Minko, I. G., Johnson, R. E., Wolfle, W. T., Harris, T. M., Lloyd, R. S., Prakash, S., and Prakash, L. (2004) Efficient and error-free replication past a minor-groove DNA adduct by the sequential action of human DNA polymerases iota and kappa. *Mol. Cell. Biol. 24*, 5687–5693.
27. Wolfle, W. T., Johnson, R. E., Minko, I. G., Lloyd, R. S., Prakash, S., and Prakash, L. (2005) Human DNA polymerase iota promotes replication through a ring-closed minor-groove adduct that adopts a syn conformation in DNA. *Mol. Cell. Biol. 25*, 8748–8754.
28. Wolfle, W. T., Johnson, R. E., Minko, I. G., Lloyd, R. S., Prakash, S., and Prakash, L. (2006) Replication past a trans-4-hydroxynonenal minor-groove adduct by the sequential action of human DNA polymerases iota and kappa. *Mol. Cell. Biol. 26*, 381–386.
29. Irimia, A., Eoff, R. L., Guengerich, F. P., and Egli, M. (2009) Structural and functional elucidation of the mechanism promoting error-prone synthesis by human DNA polymerase kappa opposite the 7,8-dihydro-8-oxo-2′-deoxyguanosine adduct. *J. Biol. Chem. 284*, 22467–22480.
30. Choi, J. Y., and Guengerich, F. P. (2008) Kinetic analysis of translesion synthesis opposite bulky N2- and O6-alkylguanine DNA adducts by human DNA polymerase REV1. *J. Biol. Chem. 283*, 23645–23655.
31. Eoff, R. L., Irimia, A., Angel, K. C., Egli, M., and Guengerich, F. P. (2007) Hydrogen bonding of 7,8-dihydro-8-oxodeoxyguanosine with a charged residue in the little finger domain determines miscoding events in *Sulfolobus solfataricus* DNA polymerase Dpo4. *J. Biol. Chem. 282*, 19831–19843.
32. Zang, H., Goodenough, A. K., Choi, J. Y., Irimia, A., Loukachevitch, L. V., Kozekov, I. D., Angel, K. C., Rizzo, C. J., Egli, M., and Guengerich, F. P. (2005) DNA adduct bypass polymerization by *Sulfolobus solfataricus* DNA polymerase Dpo4: analysis and crystal structures of multiple base pair substitution and frameshift products with the adduct 1,N2-ethenoguanine. *J. Biol. Chem. 280*, 29750–29764.
33. Choi, J. Y., Angel, K. C., and Guengerich, F. P. (2006) Translesion synthesis across bulky N2-alkyl guanine DNA adducts by human DNA polymerase kappa. *J. Biol. Chem. 281*, 21062–21072.
34. de los Santos, C., Zaliznyak, T., and Johnson, F. (2001) NMR characterization of a DNA duplex containing the major acrolein-derived deoxyguanosine adduct gamma-OH-1,-N2-propano-2′-deoxyguanosine. *J. Biol. Chem. 276*, 9077–9082.